Hindawi
Shock and Vibration
Volume 2019, Article ID 3479239, 7 pages
https://doi.org/10.1155/2019/3479239

Research Article

Chaotic Threshold for a Class of Power System Model

Xiaodong Wang,[1,2] **Zhenyong Lu**,[1] **and Caiqin Song**[3]

[1]*School of Management Science and Engineering, Shandong Normal University, Jinan 250014, China*
[2]*School of Astronautics, Harbin Institute of Technology, Harbin 150001, China*
[3]*School of Mathematical Sciences, Uiversity of Jinan, Jinan 250022, China*

Correspondence should be addressed to Xiaodong Wang; wangxd@sdnu.edu.cn and Zhenyong Lu; luzy@sdnu.edu.cn

Received 6 November 2018; Accepted 15 January 2019; Published 7 February 2019

Academic Editor: Mickaël Lallart

This paper deals with the bifurcation and chaotic dynamic characteristic of a single-machine infinite-bus (SMIB) power system under two kinds of harmonic excitation disturbance, which are induced by the external periodic load and the outer mechanical disturbance. By applying Melnikov's method, the threshold value for the occurrence of chaotic motion is provided. In addition, the chaotic boundary surface is given. The efficiency of the criteria for chaotic motion obtained in this paper is verified by bifurcation diagram, phase portraits, Poincaré section, and frequency spectrum. The results obtained in this paper will provide a better understanding of the nonlinear dynamic behaviors for this class of SMIB power system subjected to two kinds of harmonic excitation components.

1. Introduction

With the rapid development of economy and the increasing power consumption, electric power systems have become more huge and complicated. Stability problems have become more complex as interconnections become more extensive [1]. Recently, the modern power system is forced to operate close to its stability limit. Power system is exposed to disturbances of varying intensity and some of the disturbances or cascading propagation of initial disturbance. Such disturbance can lead the power system to lose its partial or total stability. Therefore, many researchers focus on the stability of electric power systems in scientific and engineering studies [2–5], especially on an equivalent single-machine infinite-bus (SMIB) power system. The model of the swing equation has attracted great interest in the last decades due to its wide application in the research of stability of such power system.

By using a random Melnikov method and numerical simulation, Wei et al. [6, 7] examined how a Gaussian white noise affects the dynamic behaviors of the power system. Zhu et al. [8] made a Hopf bifurcation analysis for a SMIB power system with subsynchronous resonance (SSR) by applying the Hopf bifurcation theorem. Nayfeh et al. [9, 10] investigated a single-machine quasi-infinite bus bar system, and they used numerical simulations to exhibit some of the complicated responses of the generator, including the period-doubling bifurcations, chaotic motions, and unbounded motions (loss of synchronism). Duan et al. [11] investigated the bifurcations associated with subsynchronous resonance of a SMIB power system with a series of capacitor compensation. Chen et al. [12] studied the chaotic control and identification problem of an SMIB power system, where the power of the machine was assumed to be a simple harmonic quantity. Moreover, Melnikov's method works effectively for discussing bifurcations of periodic orbits and homo- (hetero-) clinic orbits for dynamical systems. For instance, this method has been applied in a classical SMIB power system model [13, 14]. Zhou and Chen [15] investigated the mechanism and parametric conditions for chaotic motions of a SMIB power system, and the critical curves separating the chaotic and nonchaotic regions have been given. Chaotic and subharmonic oscillations of the SMIB power system were discussed in [16] by computing Melnikov functions with the residue of a complex function and elliptic integrals. Wang et al. [17] investigated a SMIB power system under a periodic load disturbance and obtained the threshold for the onset of chaos by using Melnikov's method.

With the development of electric power industry, a lot of new equipment has been used in the power system. For example, a valve on a steam turbine was used, which can take

quick action as a device for regulating the power of a prime mover. When the valve is under periodic perturbation, meanwhile, the system is subjected by the periodic load power, and there exists two kinds of periodic excitation. To the best of our knowledge, there are few literature considering dynamic characteristic of a single-machine infinite-bus power system under two kinds of periodic excitation disturbance. In addition, when the well-known Melnikov's method is employed to obtain the threshold value for the occurrence of chaotic motion, the analytic expressions of the homoclinic orbits need to be given. It is worth pointing out that the analytical expression of the homoclinic orbits in the mathematical model of the SMIB power system is difficult to obtain. Because of this, the mechanical power input to the synchronous machine is assumed to be a very small quantity or zero in some existing literature, which is different from the real SMIB power system in engineering practice. In this case, the original homoclinic orbits have been changed into heteroclinic obits, so the intrinsic characteristic of the original real system has been changed. Although we have investigated the nonlinear dynamic analysis of a SMIB system subjected to a periodic load disturbance before in [17], in this paper, we extend a SMIB system subjected to two kinds of disturbance. So the purpose of this paper is to investigate the bifurcation and chaotic characteristic of it. The work in this paper differs from the existing literature in two aspects: one is the two kinds of excitation components, and the other one is the way of obtaining the threshold value for the occurrence of chaotic motion by applying the Melnikov method.

2. The Formulation of a Class of SMIB Power System

In this paper, we investigate a class of single-machine infinite-bus (SMIB) power system. Figure 1 shows its configuration. In Figure 1, by using a transmission line, the synchronous machine S is transferring power to the infinite bus. We denote the equivalent main transformer of system 1 and system 2 as 3 and 4, respectively. We denote load, circuit breaker, and systematic tie line as 5, 6, and 7, respectively. In [1], the angle dynamics of the synchronous generator is described by the swing equation. So, it can be expressed as

$$\begin{cases} \dfrac{d\delta}{dt} = \Delta\omega = \omega - \omega_{\mathrm{R}}, \\ \dfrac{2H}{\omega_{\mathrm{R}}} \dfrac{d\Delta\ \omega}{dt} = P_{\mathrm{M}} - P_{\mathrm{E}}, \end{cases} \tag{1}$$

where δ is the rotor angle, ω_{R} is the synchronous angular velocity, ω is the angular speed, and $\Delta\omega$ is the angular speed deviation. $P_{\mathrm{E}}, P_{\mathrm{M}}$, and H represent the electrical power, mechanical power, and the inertia constant of the machine, respectively.

As we all know, suppose the generator is a nonsalient pole generator, and the electrical power P_{E} can be written as

$$P_{\mathrm{E}} = \frac{UE}{X} \sin\delta = P_{\mathrm{S}} \sin\delta, \tag{2}$$

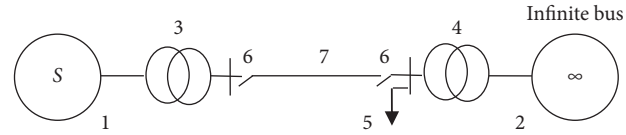

Figure 1: SMIB power system with two kinds of disturbance.

in which the reference phasor of the infinite bus bar is represented as $U\angle 0^{\circ}$, the voltage of the machine is denoted by E, and X stands for the reactance of the system.

Assume system (1) is under two kinds of disturbance: a periodic load with the amplitude P_{d} and frequency Ω_1 and an external periodic mechanical excitation disturbance with the amplitude P_{f} and frequency Ω_2. D is the damping of the synchronous generator. The following equation can be obtained:

$$\begin{cases} \dfrac{d\delta}{dt} = \omega - \omega_{\mathrm{R}}, \\ H\dfrac{d\omega}{dt} = P_{\mathrm{m}} - P_{\max}\sin\delta - D(\omega - \omega_{\mathrm{R}}) + P_{\mathrm{d}}\cos(\Omega_1 t) \\ \qquad\qquad + P_{\mathrm{f}}\cos(\Omega_2 t). \end{cases} \tag{3}$$

For the convenience of analysis, the following transforms are introduced:

$$\begin{aligned} \tau &= t\sqrt{\frac{P_{\max}}{H}}, \\ x(\tau) &= \delta(t), \\ y(\tau) &= \sqrt{\frac{H}{P_{\max}}}(\omega(t) - \omega_{\mathrm{R}}), \\ c &= \frac{D}{\omega_r\sqrt{HP_{\max}}}, \\ 0 < \rho &= \frac{P_{\mathrm{m}}}{P_{\max}} \le 1, \\ f_1 &= \frac{P_{\mathrm{d}}}{P_{\max}}, \\ \omega_1 &= \Omega_1\sqrt{\frac{H}{P_{\max}}}, \\ f_2 &= \frac{P_{\mathrm{f}}}{P_{\max}}, \\ \omega_2 &= \Omega_2\sqrt{\frac{H}{P_{\max}}}. \end{aligned} \tag{4}$$

Then, system (3) changes into

$$\begin{cases} \dfrac{dx}{d\tau} = y, \\ \dfrac{dy}{d\tau} = -\sin x - cy + \rho + f_1\cos(\omega_1\tau) + f_2\cos(\omega_2\tau). \end{cases} \tag{5}$$

In order to obtain the basic behavior of the presented SMIB system in this paper, first we study a case with no damping and no external excitation. Now let $c = 0, f_1 = 0$, and $f_2 = 0$; therefore, Equation (6) can be changed into the following form:

$$\begin{cases} \dfrac{dx}{d\tau} = y, \\ \dfrac{dy}{d\tau} = -\sin x + \rho. \end{cases} \tag{6}$$

Thus, we can obtain the equilibriums of system (6):

$$\begin{aligned} E &: (x_1, 0) = (\arcsin\ \rho, 0), \\ S &: (x_2, 0) = (\pi - \arcsin\ \rho, 0). \end{aligned} \tag{7}$$

Hence, it is easily concluded that the equilibrium $E : (x_1, 0) = (\arcsin\ \rho, 0)$ is a center, and the equilibrium $S : (x_2, 0) = (\pi - \arcsin\ \rho, 0)$ is a saddle point.

It is observed from Figure 2 that the phase portraits of the studied system (6) for different initial conditions are shown. The phase trajectory marked as circle "1" is oscillating orbits, whose angular displacement is usually smaller and the angular velocity changes its sign twice per period. At the same time, we denote the trajectory "3" as a typical rotational motion, whose angular velocity does not change its sign and its angular displacement grows with time, and we denote the trajectory "2" as the homoclinic orbit.

3. Melnikov Function of the SMIB Power System

In this section, we will study the condition for the emergence of chaotic motion in Equation (5) by applying Melnikov's method, which has been successfully applied to the analysis of chaos in many nonlinear systems [18–21].

In order to give the transversality condition by using the Melnikov's method, the SMIB system (5) is rewritten as

$$\begin{cases} \dfrac{dx}{d\tau} = y, \\ \dfrac{dy}{d\tau} = -\sin x + \rho + \varepsilon\left[-cy + f_1 \cos(\omega_1 \tau) + f_2 \cos(\omega_2 \tau)\right]. \end{cases} \tag{8}$$

Now we assume $\varepsilon = 0$, and then Hamiltonian function of Equation (8) can be given as

$$H(x, y) = \frac{1}{2}y^2 - \cos x - \rho x + H_0, \tag{9}$$

in which H_0 stands for an integral constant.

From Hamiltonian function (9), we can plot the phase portrait as shown in Figure 2. If we let $H(x_E, y_E) = 0$, it yields to

$$H_0 = \arcsin\ \rho + \cos(\arcsin\ \rho). \tag{10}$$

Therefore, the homoclinic orbit SCABS in Figure 2 is suitable for the following equation:

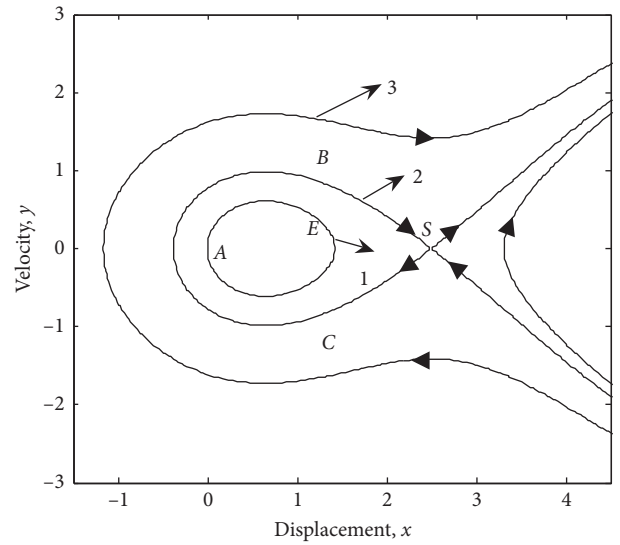

Figure 2: Phase trajectories for the unperturbed system (5).

$$\frac{1}{2}y^2 - \cos x - \rho x = \cos(\arcsin\ \rho) - \rho\pi + \rho\ \arcsin\ \rho \widehat{=} H(\rho). \tag{11}$$

We use the parametric function $[x_0(\tau), y_0(\tau)]$ to stand for the homoclinic orbit, that is,

$$\lim_{\tau \longrightarrow \pm\infty} [x_0(\tau), y_0(\tau)] = S,$$

$$y(\tau) = \pm\sqrt{2H(\rho) + 2\cos x_0(\tau) + 2\rho x_0(\tau)}. \tag{12}$$

(1) We denote $[x_0(0), y_0(0)]$ as the coordinate of point A in Figure 2, in which $y_0(0) = 0$ and $x_0(0)$ satisfy the equation $\rho x_0(0) + \cos(x_0(0)) - \rho\pi + \rho\ \arcsin\ \rho + \cos(\arcsin\ \rho) = 0$.

(2) If $\tau \in (-\infty, 0]$, we use $[x_0(\tau), y_0(\tau)]$ representing the lower part of the homoclinic orbit SCA. Contrarily, if $\tau \in [0, \infty)$, $[x_0(\tau), y_0(\tau)]$ denotes the upper part of the homoclinic orbit ABS, in which $x_0(\tau)$ and $y_0(\tau)$ are the even function and odd function, respectively.

Now, if we introduce the following notation in system (8), Equation (8) has been changed into

$$\begin{aligned} \dot{X} &= f(X) + \varepsilon g(X), \\ y &= \dot{x}, \\ X &= \begin{pmatrix} x \\ y \end{pmatrix}, \\ f(X) &= \begin{pmatrix} y \\ -\sin(x) + \rho \end{pmatrix}, \\ g(X) &= \begin{pmatrix} 0 \\ -cy + f_1 \cos(\omega_1 \tau) + f_2 \cos(\omega_2 \tau) \end{pmatrix}. \end{aligned} \tag{13}$$

With regard to the homoclinic orbit, we obtain

$$tr(Df) = \begin{pmatrix} 0 & 1 \\ -\cos(x) & 0 \end{pmatrix} = 0,$$
$$f(X(\tau)) \wedge g(X(\tau), \tau + \tau_0) = [-cy^2(\tau) + y(\tau) \cdot (f_1 \cos\omega_1(\tau_0 + \tau) + f_2 \cos\omega_2(\tau_0 + \tau))], \tag{14}$$

in which the operator $\wedge$ is defined as

$$a \wedge b = a_1 b_2 - a_2 b_1, \tag{15}$$

for any $a = (a_1, a_2)^T$ and $b = (b_1, b_2)^T$.

Therefore, the Melnikov function of Equation (8) is expressed as

$$\begin{aligned} M(\tau_0) &= \int_{-\infty}^{\infty} [f(X(\tau)) \wedge g(X(\tau), \tau + \tau_0)]\, d\tau \\ &= \int_{-\infty}^{\infty} [-cy^2(\tau) + y(\tau) \cdot (f_1 \cos\omega_1(\tau_0 + \tau) + f_2 \cos\omega_2(\tau_0 + \tau))]\, d\tau \\ &= -c\int_{-\infty}^{+\infty} y^2(\tau) d\tau + f_1 \int_{-\infty}^{+\infty} y(\tau) \cos\omega_1(\tau_0 + \tau)\, d\tau \\ &\quad + f_2 \int_{-\infty}^{+\infty} y(\tau) \cos\omega_2(\tau_0 + \tau)\, d\tau \\ &= -cK + f_1 \sin\omega_1\tau_0 I_{\text{hom1}}(\omega_1) \\ &\quad + f_2 \sin\omega_2\tau_0 I_{\text{hom2}}(\omega_2), \end{aligned} \tag{16}$$

in which

$$\begin{aligned} K &= \int_{-\infty}^{+\infty} y_0^2(\tau)\, d\tau = 2\int_0^{+\infty} y_0^2(\tau)\, d\tau \\ &= 2\int_{x_A}^{x_S} y_0(\tau)\, dx \\ &= 2\int_{x_A}^{x_S} \sqrt{2H(\rho) + 2\cos x + 2\rho x}\, dx\ , \end{aligned} \tag{17}$$

$$\begin{aligned} I_{\text{hom1}}(\omega_1) &= -2\int_0^{+\infty} y_0(\tau) \sin\omega_1\tau\, d\tau \\ &= -2\int_{x_A}^{x_S} \sin\omega_1 \cdot \left[\pm\int_{x_A}^{x} \frac{d\theta}{\sqrt{2H(\rho) + 2\cos\theta + 2\rho\theta}}\right] dx, \end{aligned} \tag{18}$$

$$\begin{aligned} I_{\text{hom2}}(\omega_2) &= -2\int_0^{+\infty} y_0(\tau) \sin\omega_2\tau\, d\tau \\ &= -2\int_{x_A}^{x_S} \sin\omega_2 \cdot \left[\pm\int_{x_A}^{x} \frac{d\theta}{\sqrt{2H(\rho) + 2\cos\theta + 2\rho\theta}}\right] dx. \end{aligned} \tag{19}$$

In Equations (12)–(14), x_A stands for the horizontal ordinate of the points A and x_S denotes the horizontal ordinates of the point S, in which the homoclinic orbit in Figure 2 intersects the x axis.

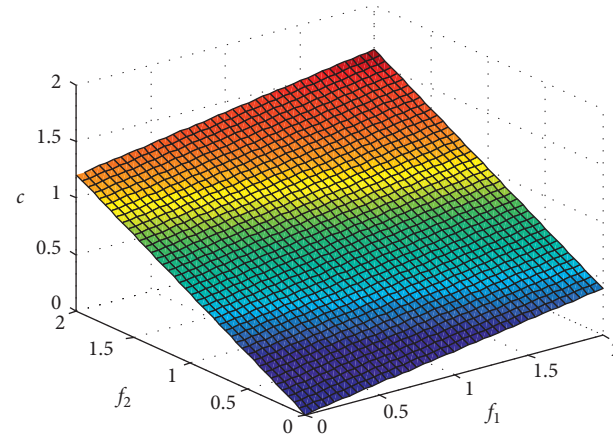

Figure 3: The boundary surface of chaotic motion.

Thus, we can see that

$$M(\tau_0) = -cK + f_1 \sin\omega_1\tau_0 I_{\text{hom1}}(\omega_1) + f_2 \sin\omega_2\tau_0 I_{\text{hom2}}(\omega_2) = 0, \tag{20}$$

has a simple zero root for $\overline{\tau}_0$ if and only if the following inequality holds

$$c < \frac{|f_1 I_{\text{hom1}}(\omega_1) + f_2 I_{\text{hom2}}(\omega_2)|}{K} = R(f_1, f_2, \omega_1, \omega_2). \tag{21}$$

The Melnikovian-detected chaotic boundary surface of equation (8) is obtained, as shown in Figure 3. When the system parameters traverse this boundary surface, the chaotic motions will be generated, i.e., in the area of $c \le R(f_1, f_2, \omega_1, \omega_2)$.

4. Numerical Simulations

In this section, numerical simulations have been conducted to verify the theoretical analysis and to better understand the changes of the dynamic characteristic for the considered SMIB power system as the periodic load and the external periodic mechanical excitation vary. We use *Dynamics* [22] to investigate the complicated dynamic behaviors of the SMIB power system by considering the bifurcation diagram. With the help of the software *Matlab*, the time histories, Poincaré maps, and frequency spectrums are plotted by using the fourth-order Runge–Kutta method. As an illustrative example, consider a specific system with the system parameters, and they are Rated MVA = 160, Rated PF = 0.85, Rated KV = 15, $\omega_R = 120\pi$, and $x'_d = 0.35$. The rest of the parameters of the SMIB power system are (converted to per unit) $M = 1$, $P_M = 0.5$, $D = 0.25$, $U = 1$, $x_T = 0.65$, and $X = x'_d + x_T = 1$. We choose parameter f_2 as a bifurcation parameter, which is corresponding to the external periodic mechanical excitation, and the other system parameters are fixed. Bifurcation diagram (Figure 4) are plotted to investigate the effects of varying the selected system parameter f_2 for typical ranges.

As the excitation amplitude f_2 increases, the rotor angle oscillation changes in terms of the sequence of period-1

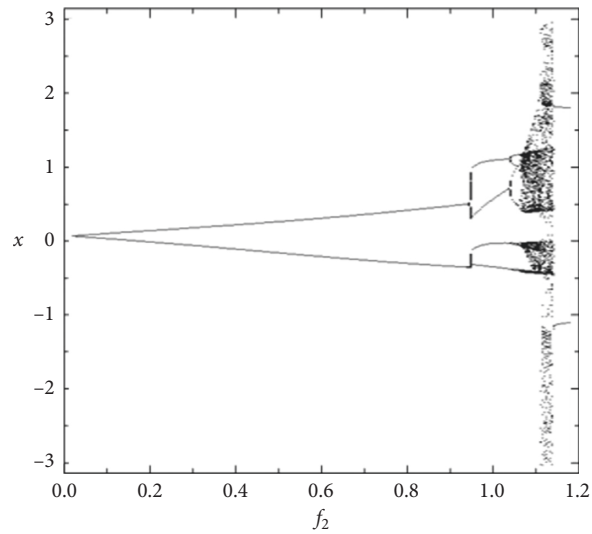

Figure 4: Bifurcation diagram with different values of parameter f_2.

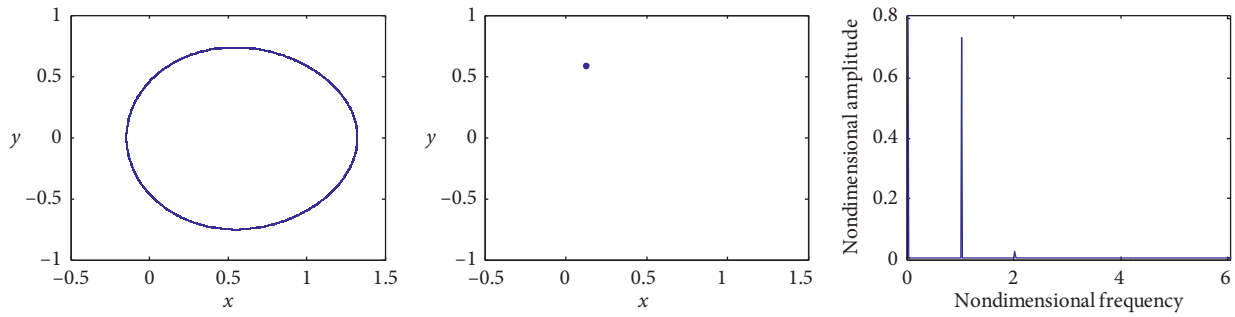

Figure 5: Dynamic response ($f_2 = 0$): (a) phase portrait; (b) Poincaré map; (c) frequency spectrum.

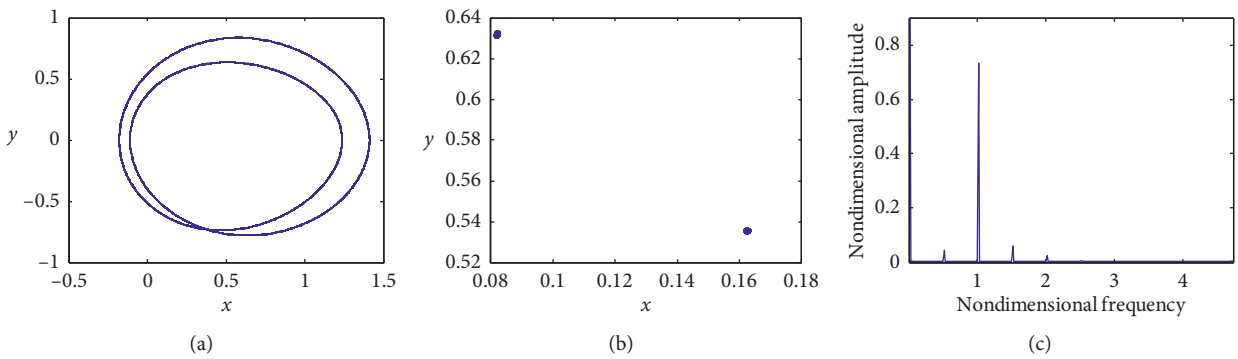

Figure 6: Dynamic response ($f_2 = 0.1$): (a) phase portrait; (b) Poincaré map; (c) frequency spectrum.

motion, period-2 motion, and chaotic motion. Figure 5 shows the phase portrait, Poincare map, and frequency spectrum of period-1 motion for $f_2 = 0$. Figures 6–8 show the phase portrait, Poincaré map, and frequency spectrum of period-2 motion for $f_2 = 0.1$, $f_2 = 0.5$, and $f_2 = 0.8$, respectively. The differences between them are the different motion forms. The reason for that lies in different excitation amplitudes. It is easily to see that the shape of the periodic trajectory subjected to two-frequency excitation becomes more complex and more irregular. Figure 9 shows the phase portrait, Poincare map, and frequency spectrum of period-4 motion for $f_2 = 1.0$. Figure 10 shows the phase portrait, Poincaré map, and frequency spectrum of chaotic motion for $f_2 = 1.1$. In the case of $f_2 = 1.1$ and the other chosen parameters, it can be easily verified that the parameter values satisfy the condition (21).

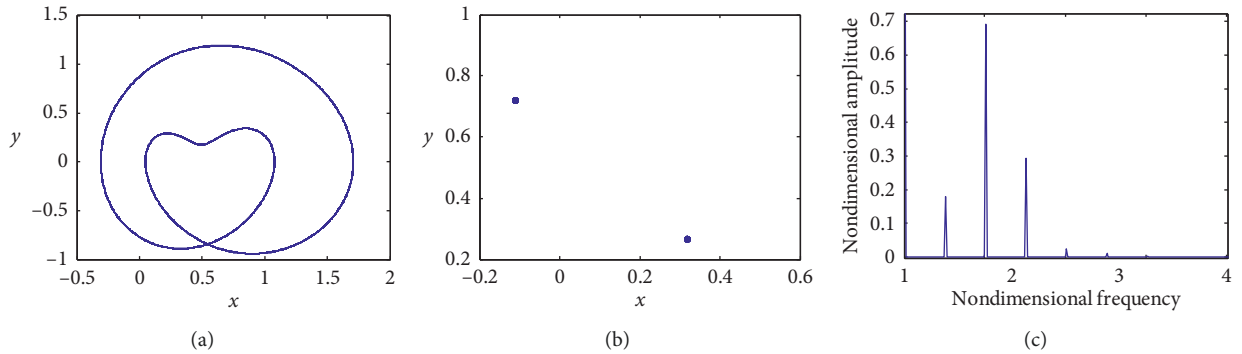

Figure 7: Dynamic response ($f_2 = 0.5$): (a) phase portrait; (b) Poincaré map; (c) frequency spectrum.

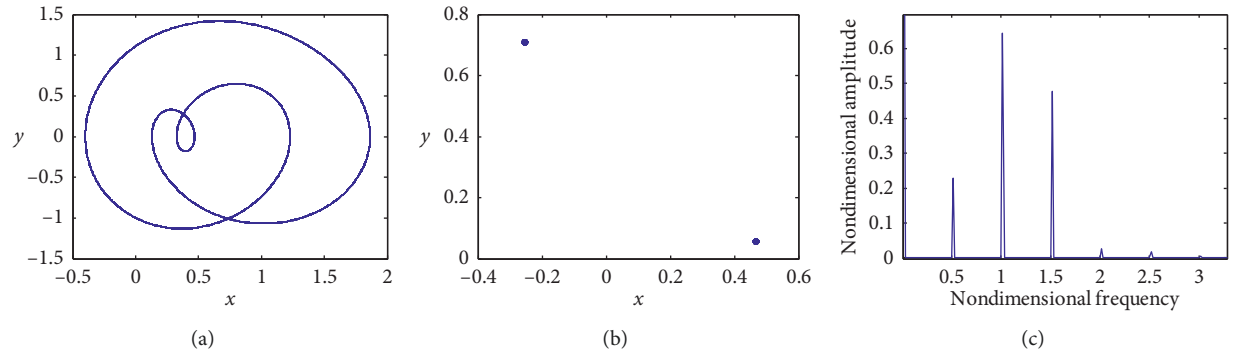

Figure 8: Dynamic response ($f_2 = 0.8$): (a) phase portrait; (b) Poincaré map; (c) frequency spectrum.

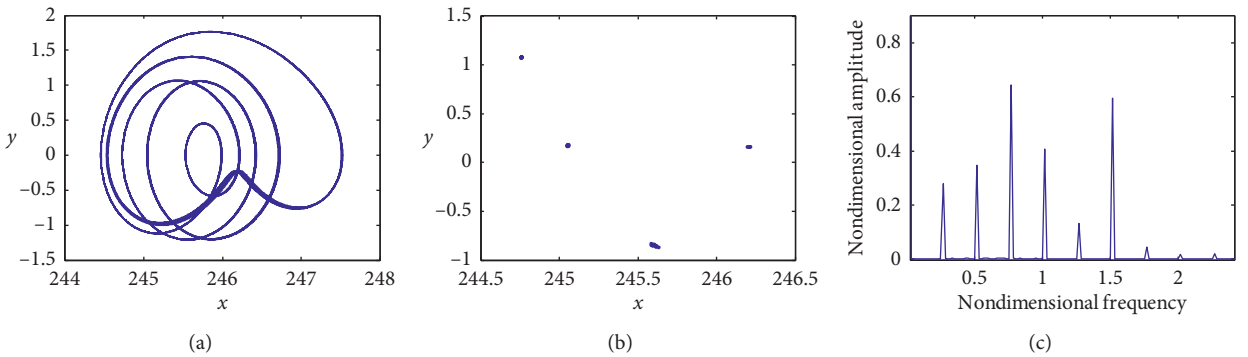

Figure 9: Dynamic response ($f_2 = 1.0$): (a) phase portrait; (b) Poincaré map; (c) frequency spectrum.

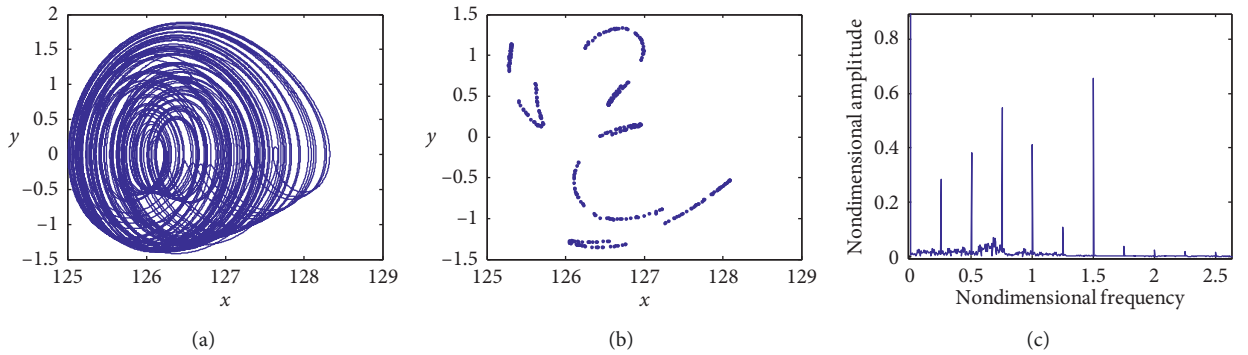

Figure 10: Dynamic response ($f_2 = 1.1$): (a) phase portrait; (b) Poincaré map; (c) frequency spectrum.

5. Conclusions

This paper has investigated the dynamical behaviors of a classical single-machine infinite-bus power system by applying theoretical analysis and numerical simulations. Our results extend the existing research by considering two kinds of excitation components, which is related to the external mechanical and electrical disturbance. With the help of phase portraits, Poincaré maps, and frequency spectrums, the transition process of different dynamic behaviors is shown. Melnikov's method is employed to give the threshold value of chaotic motion occurrence. In the considered system, there exists the phenomenon of period-doubling cascading bifurcation to chaos induced by the external excitation. These obtained results can give an overall understanding of the complex dynamic behaviors for this system.

Data Availability

The data used to support the findings of this study are available from the corresponding author upon request.

Conflicts of Interest

The authors declare that they have no conflicts of interest concerning the publication of this manuscript.

Acknowledgments

The authors would like to acknowledge the financial supports from the Higher Educational Science and Technology Program of Shandong Province, China (Grant no. J18KA235), Shandong Provincial Natural Science Foundation, China (Grant nos. ZR2018BA021, ZR2016AP06, and ZR2017PG002), and National Natural Science Foundation of China (Grant no. 11501246).

References

[1] Q. Lu and Y. Z. Sun, *Nonlinear Control of Power System*, China Science Press, Beijing, China, 1993.

[2] A. Safari, H. Shahsavari, and J. Salehi, "A mathematical model of SOFC power plant for dynamic simulation of multi-machine power systems," *Energy*, vol. 149, pp. 397–413, 2018.

[3] J. L. Jardim and A. M. Leite da Silva, "A methodology for computing robust dynamic equivalents of large power systems," *Electric Power Systems Research*, vol. 143, pp. 513–521, 2017.

[4] M. A. Mahmud, M. J. Hossain, and H. R. Pota, "Effects of large dynamic loads on power system stability," *International Journal of Electrical Power and Energy Systems*, vol. 44, no. 1, pp. 357–363, 2013.

[5] D. Groß, C. Arghir, and F. Dörfler, "On the steady-state behavior of a nonlinear power system model," *Automatica*, vol. 90, pp. 248–254, 2018.

[6] D. Q. Wei and X. S. Luo, "Noise-induced chaos in single-machine infinite-bus power systems," *EPL (Europhysics Letters)*, vol. 86, no. 5, article 50008, 2009.

[7] D. Q. Wei, B. Zhang, D. Y. Qiu, and X. S. Luo, "Effect of noise on erosion of safe basin in power system," *Nonlinear Dynamics*, vol. 61, no. 3, pp. 477–482, 2010.

[8] W. Zhu, R. R. Mohler, R. Spee, W. A. Mittelstadt, and D. Maratukulam, "Hopf bifurcations in a SMIB power system with SSR," *IEEE Transactions on Power Systems*, vol. 11, no. 3, pp. 1579–1584, 1996.

[9] M. A. Nayfeh, A. M. A. Hamdan, and A. H. Nayfeh, "Chaos and instability in a power system: subharmonic-resonant case," *Nonlinear Dynamics*, vol. 2, no. 1, pp. 53–72, 1991.

[10] M. A. Nayfeh, A. M. A. Hamdan, and A. H. Nayfeh, "Chaos and instability in a power system - primary resonant case," *Nonlinear Dynamics*, vol. 1, no. 4, pp. 313–339, 1990.

[11] X. Duan, J. Wen, and S. Cheng, "Bifurcation analysis for an SMIB power system with series capacitor compensation associated with sub-synchronous resonance," *Science in China Series E: Technological Sciences*, vol. 52, no. 2, pp. 436–441, 2008.

[12] H. K. Chen, T. N. Lin, and J. H. Chen, "Dynamic analysis, controlling chaos and chaotification of a SMIB power system," *Chaos, Solitons and Fractals*, vol. 24, no. 5, pp. 1307–1315, 2005.

[13] L. F. C. Alberto and N. G. Bretas, "Application of Melnikov's method for computing heteroclinic orbits in a classical SMIB power system model," *IEEE Transactions on Circuits and Systems I: Fundamental Theory and Applications*, vol. 47, no. 7, pp. 1085–1089, 2000.

[14] W. N. Zhang and W. D. Zhang, "Chaotic ocillation of a nonlinear power system," *Applied Mathematics and Mechanics*, vol. 20, no. 10, pp. 1175–1183, 1999.

[15] L. Zhou and F. Chen, "Chaotic dynamics for a class of single-machine-infinite bus power system," *Journal of Vibration and Control*, vol. 24, no. 3, pp. 582–587, 2016.

[16] X. W. Chen, W. N. Zhang, and W. D. Zhang, "Chaotic and subharmonic oscillations of a nonlinear power system," *IEEE Transactions on Circuits and Systems II: Express Briefs*, vol. 52, no. 12, pp. 811–815, 2005.

[17] X. Wang, Y. Chen, G. Han, and C. Song, "Nonlinear dynamic analysis of a single-machine infinite-bus power system," *Applied Mathematical Modelling*, vol. 39, no. 10-11, pp. 2951–2961, 2015.

[18] R. Tian, Y. Zhou, B. Zhang, and X. Yang, "Chaotic threshold for a class of impulsive differential system," *Nonlinear Dynamics*, vol. 83, no. 4, pp. 2229–2240, 2015.

[19] R. L. Tian, Q. L. Wu, Y. P. Xiong, X. W. Yang, and W. Q. Feng, "Bifurcations and chaotic thresholds for the spring-pendulum oscillator with irrational and fractional nonlinear restoring forces," *European Physical Journal Plus*, vol. 129, no. 5, p. 85, 2014.

[20] R. L. Tian, Y. F. Zhou, Q. B. Wang, and L. L. Zhang, "Bifurcation and chaotic threshold of Duffing system with jump discontinuities," *European Physical Journal Plus*, vol. 131, no. 1, p. 15, 2016.

[21] J. Guckenheimer and P. Holmes, *Nonlinear Oscillations, Dynamical Systems, and Bifurcations Vector Fields*, Springer-Verlag, New York, NY, USA, 1983.

[22] H. E. Nusse and J. A. Yorke, *Dynamics: Numerical Explorations*, Springer-Verlag, New York, NY, USA, 1997.